Computational Challenges of Flow Driven by Low-Head Differential in Stormwater Treatment Areas

Liqiong Zhang, Jie Zeng, and Emile Damisse

Figure 1. Location of the stormwater treatment area-3/4 (SFWMD, 2014).

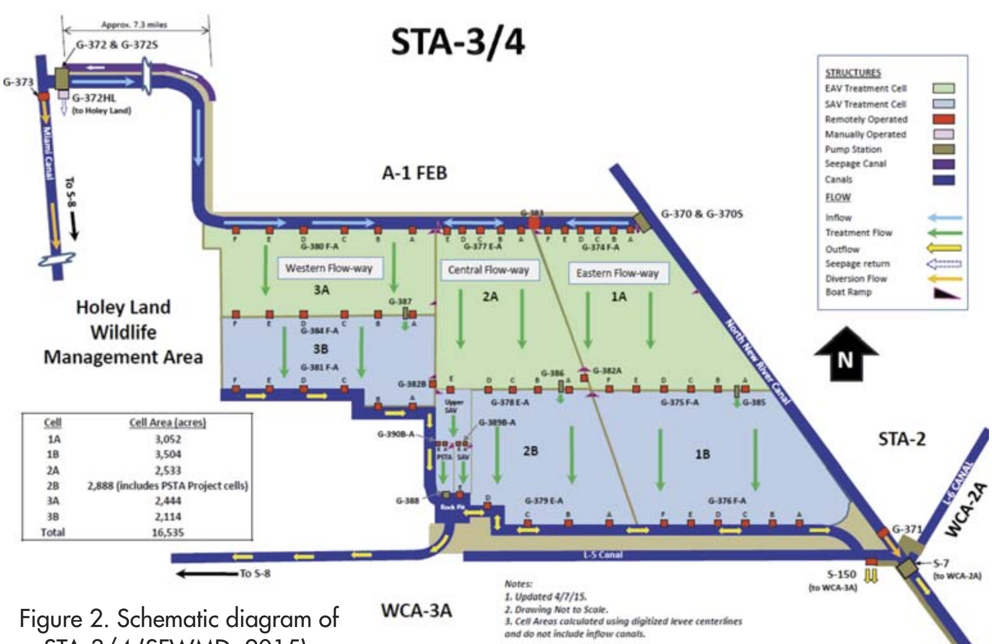

Figure 2. Schematic diagram of STA-3/4 (SFWMD, 2015).

Liqiong Zhang and Jie Zeng are lead engineers, and Emile Damisse is section lead in the Hydrology and Hydraulic Bureau of South Florida Water Management District in West Palm Beach.

The South Florida Water Management District (District) operates over 500 hydraulic structures (pumps, spillways, culverts, and weirs) for water resources management in a 46,439-sq-km (~17,930-sq-mi) region. Accurate flow estimation for these hydraulic structures is a key component to environmental flow in stormwater treatment areas (STAs) prior to its release to the Everglades, one of only three wetland areas of global importance. Culverts have been extensively designed and constructed for water divergence, drainage, and water quality control in the STAs.

Stormwater Treatment Area 3/4 (STA-3/4) is one of the six STAs constructed to reduce total phosphorus (TP) from the Everglades Agricultural Area (EAA) and Lake Okeechobee. A regional map (Figure 1) shows that STA-3/4 is located in the boundary of Palm Beach County and Broward County, bordered by Holey Land Wildlife Management Area on the west and the Water Conservation Area 3A (WCA-3A) on the south (SFWMD, 2007).

Accurate water budget analysis of STA-3/4 is a key to evaluating the performance of this STA on TP reduction. In this study, the procedures of annual water budget analysis are:

1) Improvement of rating equations of internal structures with the aid of computational fluid dynamics (CFD) simulation
2) Filtering of white noise in water stages
3) Verification of water budget and flow distributions
4) Providing basic information for evaluating performance of STA-3/4

Since October 2003, the inflow structures have been operating and conveyed the runoff/drainage from the EAA and Lake Okeechobee releases into STA-3/4.

The STA-3/4 has three flow-ways: eastern, central, and western. The eastern flow-way consists of two consecutively linked cells 1A and 1B, the central flow-way consists of two consecutively linked cells 2A and 2B, and the western flow-way consists of two consecutively linked cells 3A and 3B. The following flows were noted:

- Inflow to the eastern flow-way is controlled by six gated concrete-box culverts (G-374 A–F)
- Outflow from cell 1A and inflow into cell 1B are through six gated concrete-box culverts (G-375 A–F)
- Inflow to the central flow-way is controlled by five gated concrete-box culverts (G-377 A–E)
- Outflow from cell 2A and inflow into cell 2B are through five gated concrete-box culverts (G-378 A–E)
- Inflow to the western flow-way is controlled by six gated concrete-box culverts (G380 A–F)
- Outflow from cell 3A and inflow into cell 3B are through six gated concrete-box culverts (G-384 A–F).

The District's flow ratings are validated and calibrated with data comprising field measurements of discharge, and water stages and operational settings are monitored in near real time. The goal of improving flow ratings at hydraulic structures relies highly on field flow measurements collected by acoustic flow meters and supplemented by three-dimensional CFD, especially for complex hydraulic structures and/or extreme hydrologic events. However, the monitoring data show that most of the internal culverts in STA-3/4 are frequently subject to low-head differential. A histogram analysis shows that low-head differential (≤±0.05 ft) occurred at 62.23 percent, 56.78 percent, and 73.74 percent of the period of record at G-375A-F, G-378A-E, and G-384A-F, respectively. This high occurrence of low-head differential would explain the abnormally high residuals in the relevant cell-based water budgets, which makes it difficult to evaluate the performance of individual treatment cells. Due to the detection limit of stage sensors and other factors, such as wind surge, uncertainties in the monitored low-head differential are considerable, which would propagate into the rated flows as one of the inputs in the rating equation.

An approach integrating CFD and filtering techniques was investigated to improve the rated flows at these local internal culverts in STA-3/4. First, accurate flow rating at local structures under low-head differential was obtained by using the flow data generated by CFD with special treatment. By doing so, the calibrated rating would not be contaminated by the measurement uncertainty in low-head differential. Second, low-pass filter of signal process and LOWESS were utilized, respectively, to remove the white noise in the water stages due to instrument resolution and wind effects. The time series of water stages filtered with low-pass filter and LOWESS, respectively, were input in flow computation at the internal culverts of STA-3/4. Finally, water budget analysis was conducted for the relevant treatment cells with the new computed flows at the internal culverts. The water budget residuals were decreased substantially after stage filtering compared with those before stage filtering. The proposed methodology for water budget improvement of STA-3/4 can be applied to other hydrologic and hydraulic analyses.

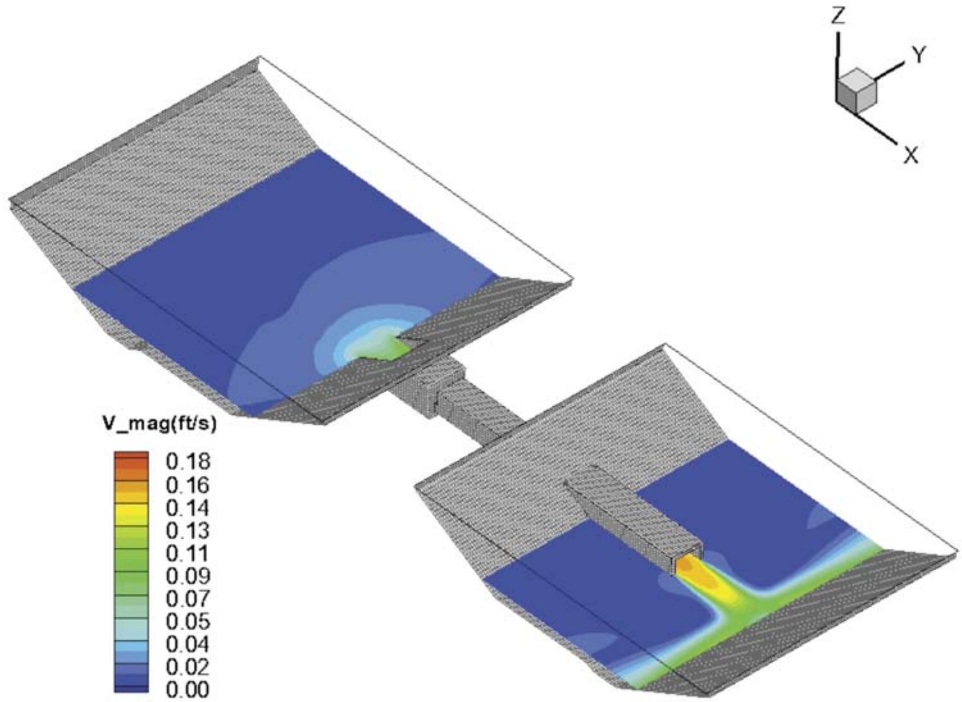

Figure 3. CFD Simulation for G-384C under low-head differential.

Table 1. Rating calibration of culvert G-384C

Head Water Stage (ft)	Tail Water Stage (ft)	Gate Opening (ft)	CFD-simulated Discharge (cfs)	Rated Discharge (cfs)	|Percent Error|
10.220	10.200	1.300	11.25	11.37	1.04%
11.840	11.800	1.700	20.94	21.41	2.24%
11.280	11.200	7.500	137.44	123.84	9.89%
11.600	11.500	4.000	86.61	83.71	3.35%
11.700	11.650	1.150	15.54	15.78	1.53%
12.200	12.170	6.000	72.43	65.66	9.35%
11.500	11.490	5.000	36.02	32.66	9.34%
11.060	11.000	2.400	37.85	38.00	0.39%
				Mean	**4.64%**

Methology

Flow Rating Using Computational Fluid Dynamics Techniques

Using the CFD technique with special treatment, flow rating under low-head differential was investigated for culverts G384A-F. The calibrated discharge coefficient for full pipe flow under low-head differential is 0.715 (less than 0.754), which was calibrated under normal ranges of head differential. Therefore, it indicates that the calibrated rating parameters for low-head differential might be considerably dif-

Continud on page 34

Continued from page 33
ferent from those under normal ranges of head differential. In the CFD simulation shown in Figure 3, the setup boundaries are listed as: all solid boundaries of the computational domain, including channel bottom; gate surface and culvert barrel were simulated as no-slip surface; the inlet and outlet boundaries were specified as the water stages; and the water surface was specified as free-surface boundary with volume of fluid.

Before CFD simulation, an analysis was conducted to investigate the conjunction frequencies at which the headwater stage, tailwater stage, and gate opening occurred in the overall period of record. Based on the frequency analysis, eight different combinations of hydrologic condition (headwater stage and tailwater stage) and operation condition (gate openings) were selected and used for CFD simulation to represent the most likely flow conditions at this culvert group.

Thus, the CFD-simulated flow data were applied in the rating calibration under low-head differential, yielding more reliable and accurate rating with the least measurement uncertainty in water stages.

The full pipe flow equation for culvert (SFWMD, 2009) is stated as:

$$Q = C_d A_0 \sqrt{\frac{2g(H-h)}{\left(\frac{A_0}{A_G}\right)^2 + 2C_d^{\,2}\left(1 - \frac{A_0}{A_G} + \frac{gn^2 L}{(1.49)^2 R_0^{4/3}}\right)}} \quad (1)$$

where Q is the discharge through each of the culvert barrels, H is the headwater elevation upstream of the culvert entrance (an approximation of the energy head by neglecting the approach velocity), h is the tailwater elevation at the culvert exit, L is the barrel length, n is the Manning roughness coefficient, g is gravitational acceleration, A_0 is the full-pipe area, A_G is the area under the gate opening, R_0 is the full-pipe hydraulic radius, and C_d is the discharge coefficient for full pipe flow.

The rating parameters, including C_d and n for full pipe flow, were determined through nonlinear regression techniques applied to CFD-simulated flow data. Here, the discharge coefficient and Manning's friction coefficient were calibrated as 0.715 and 0.012, respectively, for full pipe flow. The computed discharges with the new rating and CFD-simulated discharges are provided in Table 1 and shown in Figure 4. There is agreement between the CFD-simulated and rated discharges, with 4.64 percent (from 0.39 to 9.89 percent) of averaged absolute relative error.

By using the CFD techniques, a reliable flow rating at local structures was obtained, which would not be subject to measurement uncertainties in low-head differential. However, the white noise in water stages needs to be removed before the reliable flow rating is applied to compute flow at local structures. Here, two approaches, including low-pass filtering and LOWESS, were used to filter the noise in the monitored water stages, respectively.

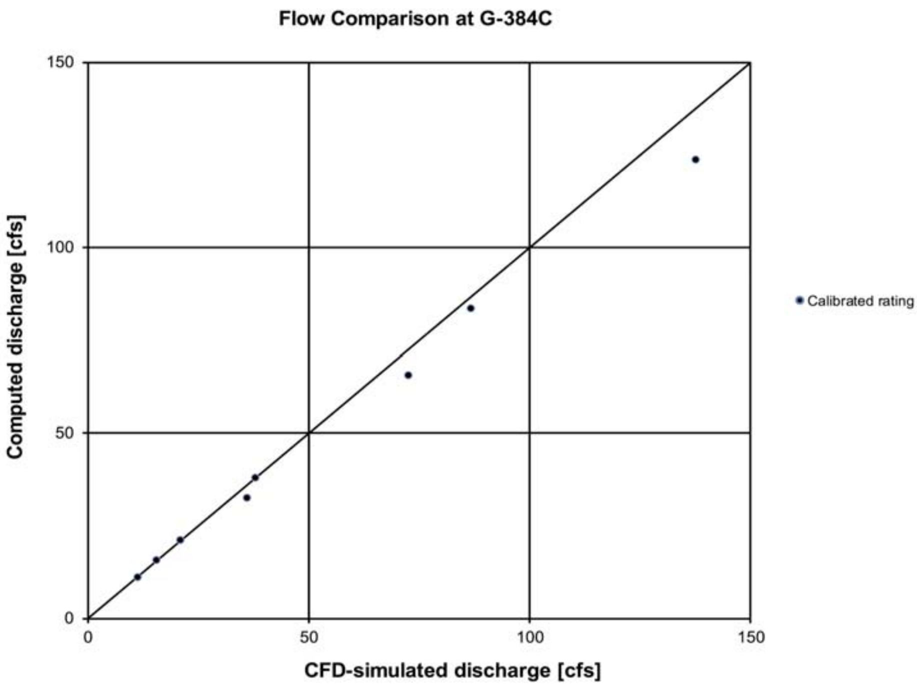

Figure 4. Comparison between CFD-simulated and computed discharges at G-384C.

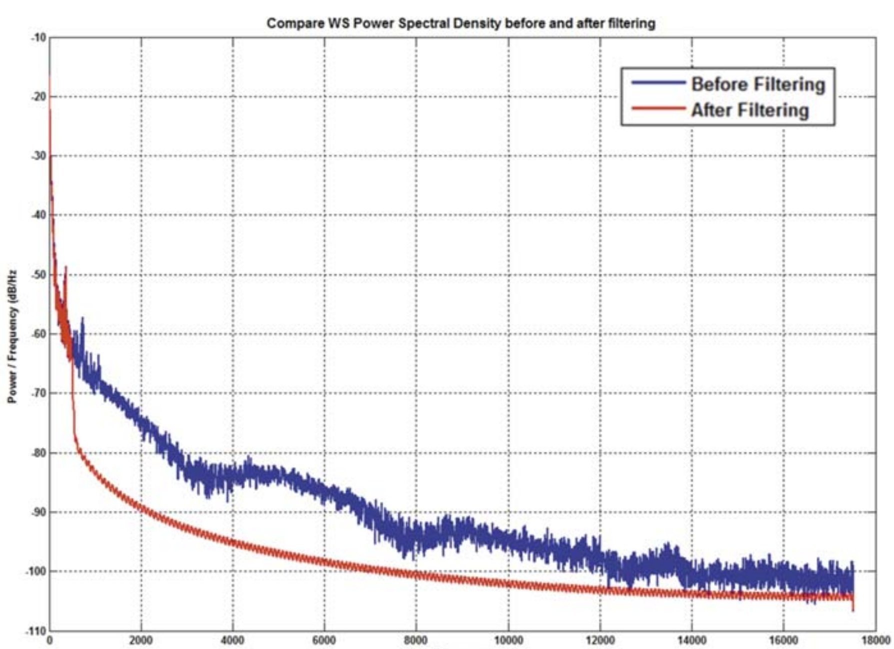

Figure 5. Spectrum of G-375D-H (one-minute interval data) for WY 2008: (i) before filtering (shown in blue), and (ii) after applying Type I Chebyshev low-pass filtering (shown in red).

Water Stage Filtering With Low-Pass Filter

The Chebyshev filter for low-pass filtering was used to filter high-frequency noise from stage data by convolving the spectrum of the time series obtained using the Chebyshec filter, which is given as:

$$T_N(\Omega) = \cos(N\cos^{-1}(\Omega)), \qquad |\Omega| \le 1$$
$$= \cosh(N\cosh^{-1}(\Omega)), \qquad |\Omega| > 1 \tag{2}$$

Here, Type *I* Chebyshev was used for filtering the water stage, which has the magnitude response

$$\left| H_a(j\Omega)\right|^2 = \frac{1}{1+\varepsilon^2 T_N^2(\Omega/\Omega_P)} \tag{3}$$

where N is the filter order, ε is a user-supplied parameter that controls the amount of pass-band ripple, and Ω_P is the upper pass band edge.

The routine used for the data set takes the spectrum, as shown in Figure 5. The filtered and unfiltered one-minute interval headwater stages at culvert G-375D are shown in Figure 6.

Then, with the calibrated rating equation, flows through the internal culverts were calculated with the filtered water stages and monitored operational settings.

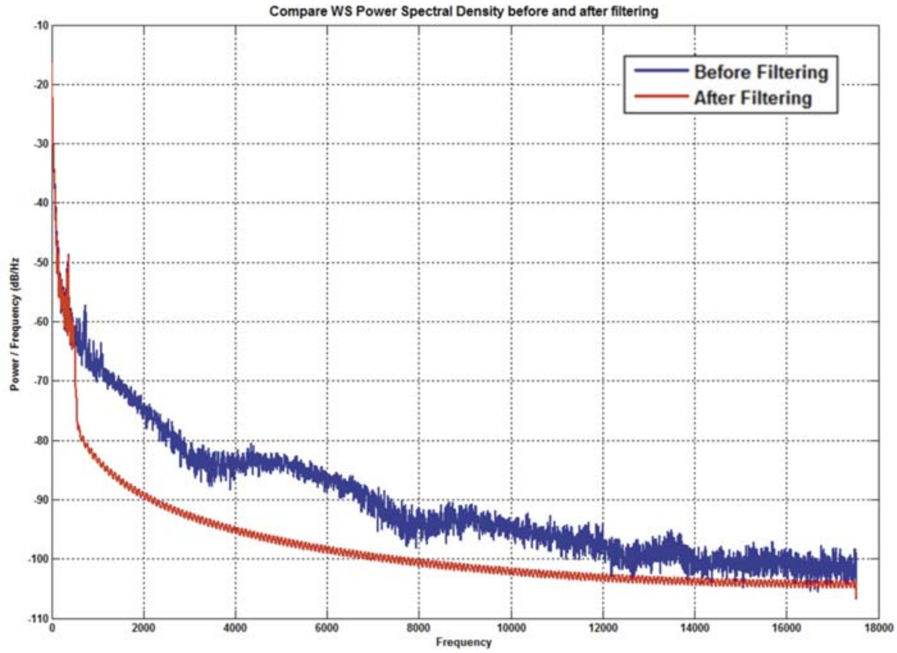

Figure 6. One-minute interval headwater stage hydrograph at G-375D for WY 2008: (i) before filtering (black line), and (ii) after low-pass filtering (red line).

Water Stage Filtering With LOWESS

There are several types of nonparametric regression. The most commonly used is the LOWESS procedure, which was first developed by Cleveland (1979). Here, LOWESS was used to filter the water stages, as shown in Figure 7.

Also, flows through the internal culverts were calculated with the water stages filtered with LOWESS and the monitored operational settings. These flows through internal culverts are inflows or outflows for individual cells, which will be applied to the water budget analysis in the following section.

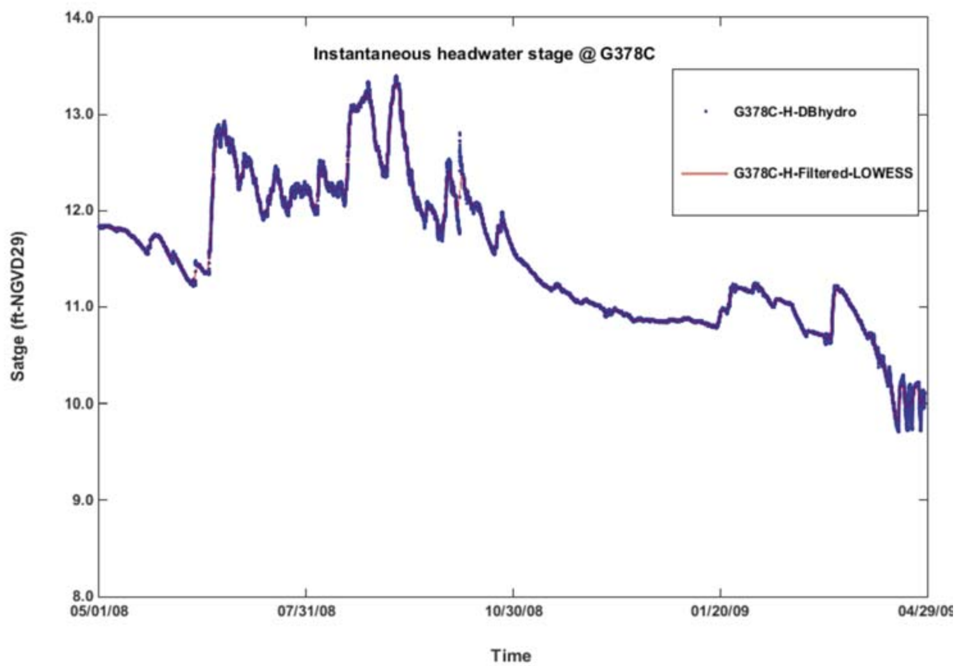

Figure 7. One-minute interval headwater stage hydrograph at G-378C for WY 2009: (i) before filtering (blue dot), and (ii) after LOWESS filtering (blue line).

Water Budget Analysis

In order to evaluate the performance of each cell and entire STA on TP reduction, water budget analysis was conducted using the calculated flows obtained by the proposed methodology. The objective is to verify whether the proposed mythology integrating CFD and stage filtering can help to reduce the residuals of cell-based water budgets.

For simplification, only the inflow and outflow are counted in the water balance equation as follows:

$$I - O = \Delta S / \Delta T \tag{4}$$

where *I* is the inflow, *O* is the outflow, ΔS is the storage change, and ΔT is the time period.

The precipitation changes in storage and evapotranspiration are negligible based on the past experiences with STA-3/4. The seepage needs further investigation and is beyond the scope of this study. Thus, the residual of the water budget here only reflects the difference between the total inflow and the total outflow within a water year. Tables 2 and 3 list the results of the WY2006 water budget.

It can be seen from Tables 2 and 3 that the residuals of the cell-based water budgets were significantly reduced through the low-pass filtering or LOWESS filtering.

Results

Using the proposed mythology, cell-based water budget analysis was conducted involving three internal culvert groups, including G-375A-F, G-378A-E, and G-384A-F for the

Continud on page 36

Table 2. WY2006 water budget for cell 2A and 2B in STA-3/4 with low-pass filtering.

Before filtering

Cell#	Inflow (ac-ft)					Outflow (ac-ft)						Residual= Outflow - inflow	
2A	G377A	G377B	G377C	G377D	G377E	G378A	G378B	G378C	G378D	G378E			
	39908.67	39469.98	40591.89	58161.7 8	50132.94	98579.23	99979.81	100672.3	72458.85	10596.93		154021.83	50.45%
2B	G378A	G378B	G378C	G378D	G378E	G379A	G379B	G379C	G379D	G379E	G388		
	98579.23	99979.81	100672.3	72458.85	10596.93	64856.45	63632.01	64381.39	68198.80	8.27		-121210.19	-37.68%

After filtering

Cell#	Inflow (ac-ft)					Outflow (ac-ft)						Residual= Outflow - inflow	
2A	G377A	G377B	G377C	G377D	G377E	G378A	G378B	G378C	G378D	G378E			
	39908.67	39469.98	40591.89	58161.78	50132.94	70670.01	72296.12	72435.06	35994.99	10209.59		33340.50	13.61%
2B	G378A	G378B	G378C	G378D	G378E	G379A	G379B	G379C	G379D	G379E	G388		
	70670.01	72296.12	72435.06	35994.99	10209.59	64856.45	63632.01	64381.39	68198.80	8.27		-528.85	-0.20%

Table 3. WY2006 water budget for cell 2A and 2B in STA-3/4 with LOWESS filtering.

Before filtering

Cell#	Inflow (ac-ft)					Outflow (ac-ft)						Residual= Outflow - inflow	
2A	G377A	G377B	G377C	G377D	G377E	G378A	G378B	G378C	G378D	G378E			
	39908.67	39469.98	40591.89	58161.7 8	50132.94	98579.23	99979.81	100672.3	72458.85	10596.93		154021.83	50.45%
2B	G378A	G378B	G378C	G378D	G378E	G379A	G379B	G379C	G379D	G379E	G388		
	98579.23	99979.81	100672.3	72458.85	10596.93	64856.45	63632.01	64381.39	68198.80	8.27		-121210.19	-37.68%

After filtering

Cell#	Inflow (ac-ft)					Outflow (ac-ft)						Residual= Outflow - inflow	
2A	G377A	G377B	G377C	G377D	G377E	G378A	G378B	G378C	G378D	G378E			
	39908.67	39469.98	40591.89	58161.78	50132.94	70474.02	72071.59	72216.69	72239.85	10166.21		68903.09	26.23%
2B	G378A	G378B	G378C	G378D	G378E	G379A	G379B	G379C	G379D	G379E	G388		
	70474.02	72071.59	72216.69	72239.85	10166.21	64856.45	63632.01	64381.39	68198.80	8.27		-36091.44	-12.93%

Continued from page 35

whole period of record. Most of the residuals with the proposed methodology were decreased significantly. However, there are still some exceptional cases where the residuals were not significantly lower than those without stage filtering. Therefore, it can be tentatively concluded that the proposed mythology is promising, but still needs more effort and investigation to improve.

References

- Cleveland, William S. (1979). "Robust Locally Weighted Regression and Smoothing Scatterplots". *Journal of the American Statistical Association*, 74 (368): 829–836. doi:10.2307/2286407.
- SFWMD (2007). “STA 3/4 Operation Plan.” South Florida Water Management District, West Palm Beach, Fla.
- SFWMD (2009). “Atlas of Flow Computations at Hydraulic Structures in the South Florida Water Management District.” South Florida Water Management District, West Palm Beach, Fla.
- SFWMD (2014). Retrieved from http://my.sfwmd.gov/portal/page/portal/operations%20and%20maintenance%20resources/portlets/sta%20maps/staregionalmap_fig5.1_2014_final_1.jpg.
- SFWMD (2015). Retrieved from http://my.sfwmd.gov/portal/page/portal/operations%20and%20maintenance%20resources/portlets/sta%20maps/sta34_april_7_2015_with_table.pdf.